Laser single-shot magnetization reversal in $Co_{1-x}Lu_x$ nanostructures

Y. Peng, G. Malinowski, W. Zhang, D. Lacour, F. Montaigne, S. Mangin, and M. Hehn*
Université de Lorraine, CNRS, Institut Jean Lamour, F-54000 Nancy, France

(Received 25 April 2023; accepted 26 May 2023; published 12 June 2023)

The magnetic properties of Pt/$Co_{1-x}Lu_x$/Pt thin films have been investigated. For an alloy thickness of 3 nm, the saturation magnetization linearly decreases from 830 kA/m to 400 kA/m for x varying between 18% and 40%, including the proximity-induced moment in platinum. Furthermore, we show that $Co_{1-x}Lu_x$ alloys 3 nm thick thin films have a perpendicular magnetic anisotropy for a concentration ranging between 25% and 40%. A single femtosecond laser shot leads to a demagnetized state with a domain size that increases with the decrease of saturation magnetization. Patterning the layer into dots leads to a single domain structure that can be fully reversed using a single laser pulse. The statistics and the origin of the nondeterministic reversal are discussed based on the atomistic model.

DOI: 10.1103/PhysRevB.107.214415

I. INTRODUCTION

The ultrafast magnetization reversal in picosecond timescales induced by femtosecond laser pulses or all optical switching (AOS) of magnetization is at the heart of current developments in femtomagnetism. Multiple-pulse helicity dependent [all optical helicity-dependent switching] [1–3] or single-pulse helicity independent [all optical helicity-independent switching (AO-HIS)] [4–9] deterministic reversal could be observed in thin films or nanostructures, without any applied field or current. AO-HIS is mainly observed in gadolinium-based rare earth (RE)/transition metals (TMs) ferrimagnetic alloys or multilayers. Only recently was it observed in materials without gadolinium—namely, the ferrimagnet Mn_2Ru_xGa [8] and the ferrimagnetic multilayer [Co/Tb] [9]. In the case of gadolinium-based alloys, models are able to reproduce such behaviors when considering two antiferromagnetically exchange coupled magnetization sublattices and different relaxation times for each sublattice [5,10]. In this respect, in most materials, gadolinium seems to be a key ingredient, considering its low relaxation time that arises from the small spin-orbit coupling of gadolinium (with $L = 0$) [11] and its antiferromagnetic coupling to TMs. The theoretical results also suggest that engineering the element-specific damping in the alloy can open up new classes of materials that exhibit low-energy, ultrafast AO-HIS [12]. Searching for other RE having a low orbital angular momentum as in gadolinium ([Xe].4f7.5d1.6s2), only lutetium ([Xe].4f14.5d1.6s2) and lanthanum ([Xe].4f0.5d1.6s2) also possess $L = 0$, and furthermore $S = J = 0$. First of all, in both cases, only few publications have reported on their magnetic properties. Second, no test of AO-HIS has been done on $TM_{1-x}Lu_x$ or $TM_{1-x}La_x$ up to now.

The crystallographic and magnetic properties of $Co_{1-x}Lu_x$ have been studied in the past. Paramagnetic behavior was observed for $CoLu_3$, Co_3Lu_4, and Co_2Lu, while ferromagnetism was observed for Co_3Lu and $Co_{17}Lu_2$ [13]. A partial substitution of aluminum for cobalt in Co_2Lu leads at first (partial concentration of aluminum <0.08) to an exhibition of itinerant metamagnetism, and then to the appearance of ferromagnetism [14]. In the case of $Fe_{1-x}Lu_x$ alloys, magnetization measurements, between 2 K and 850 K, of Fe_2Lu, Fe_3Lu, $Fe_{23}Lu_6$, and $Fe_{17}Lu_2$ showed the ferromagnetic character, and $Fe_{17}Lu_2$ has a particular behavior: it is ferromagnetic below 100 K and, at 270 K, the magnetization in a 100-Oe field shows a peak characteristic of a Néel temperature. The transition therefore occurs between a ferromagnetic state and an antiferromagnetic state. On the other hand, measurements at 300 K [15] using x-ray magnetic circular dichroism showed that Fe_2Lu is ferrimagnetic. In this case, the magnetic moment of lutetium is carried by the 5d-electrons and is antiparallel to the iron 3d moment [16]. The magnetic moment of lutetium ($\mu_{Lu} = -0.41\ \mu_B$) is much weaker than the one of iron ($\mu_{Fe} = 1.63\ \mu_B$). It is therefore not possible to reach the magnetic compensation at room temperature. Nevertheless, the magnetization in $(FeCo)_xGd_{1-x}$ alloys has been reversed using a single pulse even in the CoFe-dominant phase and far from the magnetic compensation [17]. In this work, we investigate and optimize the magnetic properties of $Co_{1-x}Lu_x$ to test whether AO-HIS occurs in this material. Indeed, a necessary prerequisite for our study is the achievement of perpendicular-to-film-plane magnetization at zero applied field, or perpendicular magnetic anisotropy (PMA). The latter is more easily obtained with a Co/Pt interface when the thickness of the layer is thin.

II. EXPERIMENTAL DETAILS

Glass/Ta(5)/Pt(4)/$Co_{1-x}Lu_x$(3)/Pt(2) (thickness in nanometers) alloy layers were grown by rf (cobalt) and dc (tantalum, platinum, lutetium) magnetron sputtering in an AJA sputtering tool with a base pressure lower than 3×10^{-8} mbar. The transparent glass substrate was used for the

*michel.hehn@univ-lorraine.fr

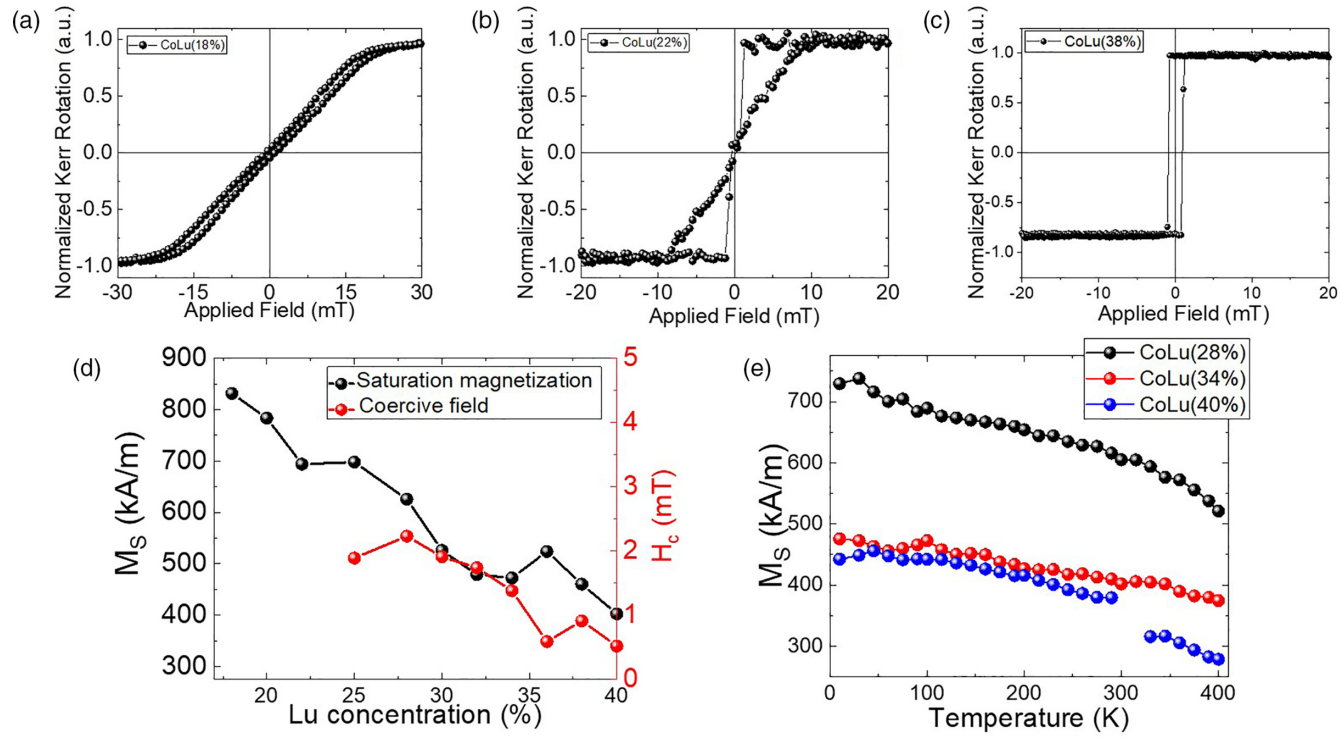

FIG. 1. Typical Kerr rotation hysteresis loops for three different compositions of lutetium: (a) 18%, (b) 22%, and (c) 38%. (d) Variation of the saturation magnetization and coercive field versus the lutetium concentration. (e) Variation of the saturation magnetization versus temperature for $Co_{1-x}Lu_x$ alloys with concentrations of 28%, 34%, and 40%.

pump/probe geometry; the Ta(5)/Pt(4) buffer layer and Pt(2) capping layer are used to promote perpendicular-to-film-plane magnetization in $Co_{1-x}Lu_x$. The top platinum layer also acts as a protecting layer against oxidation. The lutetium concentration was varied between 18% and 40%. The magnetic properties have been checked using a Kerr rotation magnetometer using a continuous He-Ne laser with a wavelength of 633 nm, and a vibrating sample magnetometer (to get the saturation magnetization). Linearly polarized femtosecond laser pulses of time duration 50 fs and with a central wavelength of 800 nm (1.55 eV) were used. Samples were observed with a tabletop differential polar MOKE microscope using a light-emitting diode (center wavelength ~630 nm) as a light source.

Typical hysteresis loops measured in the polar MOKE configuration with a field applied perpendicular to the film plane for different lutetium concentrations are reported in Fig. 1. For a lutetium concentration lower than 20%, the magnetization lies in the sample plane. A special case could be observed for a lutetium concentration of 22%, for which a perpendicular-to-film-plane multidomain-like hysteresis curve could be measured [18]. For concentrations above 22%, the hysteresis loops are square with a remanence equal to one, evidence of PMA. As shown in Fig. 1(d), the saturation magnetization, M_s, calculated using the nominal $Co_{1-x}Lu_x$ thickness and the sample surface linearly decreases from 830 kA/m at 18% to 400 kA/m at 40%. This effective value of M_s includes the moment induced in platinum through proximity effects. Indeed, element-resolved x-ray magnetic measurements done in multilayers of platinum and RE:3*d* TM ferrimagnetic alloys showed that the proximity-induced moment in platinum was parallel to the TM sublattice rather than the RE or the net moment [19]. Considering the low thickness of the $Co_{1-x}Lu_x$ layer, the contribution of platinum to the total magnetic moment must be significant.

Finally, the variation of the saturation magnetization versus temperature for $Co_{1-x}Lu_x$ alloys with a concentration of 28%, 34%, and 40% clearly shows that, for temperatures ranging between 0 K and 400 K, the saturation magnetization monotonously decreases without depicting the presence of a magnetic compensation [Fig. 1(e)]. Considering the higher moment of cobalt with respect to lutetium, all samples are cobalt dominant. This trend is similar to the one observed in the Fe_2Lu compounds [16]. Indeed, considering that the magnetic moment of lutetium ($\mu Lu = -0.41\ \mu_B$), is much weaker than the one of iron ($\mu Fe = 1.63\ \mu_B$), it is not possible to reach the magnetic compensation. A measure of a sample with 50% of lutetium showed no magnetic response at room temperature—meaning, that for this concentration, the Curie temperature is below room temperature.

Single-shot reversal experiments have been performed on all full-film samples with PMA (Fig. 2). The lower critical fluence for which domains appear is 2.1 mJ/cm^2, while the upper fluence limit for which the samples burn out is ~27.1 mJ/cm^2. In Fig. 2, we report the typical evolution of the domain size for a fluence fixed to 6.7 mJ/cm^2; the same trend has been observed for fluences between 2.1 mJ/cm^2 and 27.1 mJ/cm^2. From the domain structure analysis, no sign of single-shot reversal could be extracted. A possible reason could be that domains are smaller than the spot size. Indeed, the observation

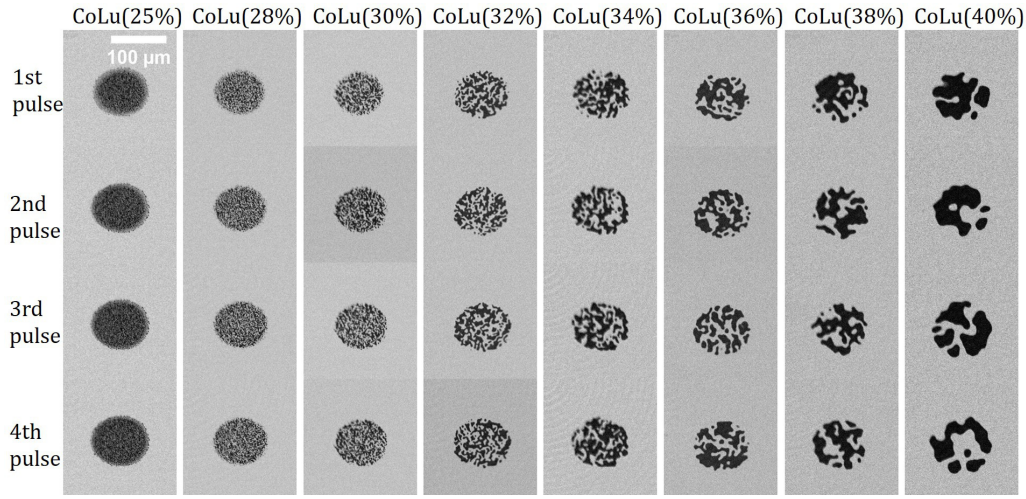

FIG. 2. Domain structure stabilized after 50-fs laser pulses with fluence 6.7 mJ/cm^2. The images are subtracted by the background, which is saturated by a magnetic field. From left to the right, increasing the lutetium concentration. From top to the bottom, 1 pulse, 2 pulses, 3 pulses, and 4 pulses.

of AOS requires that the equilibrium size of magnetic domains forming during the cooling process should be larger than the laser spot size [20]. However, a clear increase in the domain size occurs when the lutetium content increases from 25% to 40%. This result can be attributed to the decrease of the saturation magnetization as expected from domain theory in materials with PMA [21].

While a mean domain size is very difficult to extract from Fig. 2, we have chosen to measure the total length of the domain walls. An increase of the domain wall length is obviously associated with a decrease in domain size. The result of the total domain perimeter, averaged over the states obtained for four pulses, is given in Fig. 3. As expected, a decrease of saturation magnetization leads to a decrease in the domain wall perimeter. Using the expression of the domain period in parallel stripe domains [21], we estimated theoretically the domain wall length in a circle of 95 μm in diameter (the size of the region where domains are stabilized after the laser pulse shot). Therefore, the thickness was fixed to 3 nm and M_s was varied from 700 to 400 kA/m. Using the dependence of exchange on the saturation magnetization for a ferromagnet, $\frac{A(\%\mathrm{Lu})}{A(0)} = \left(\frac{M_s(\%\mathrm{Lu})}{M_s(0)}\right)^2$ [22,23], and since the domain wall energy scales as $\sqrt{A(\%\mathrm{Lu})}$, a linear variation of the domain wall energy with saturation magnetization was taken into account: $\sigma_W(M_s) = \sigma_W(400)\frac{M_s}{400}$ ($\sigma_W(400) = 0.23$ J/m^3). Considering the very crude approximation made in our model, a good agreement between theory and experiments could be obtained.

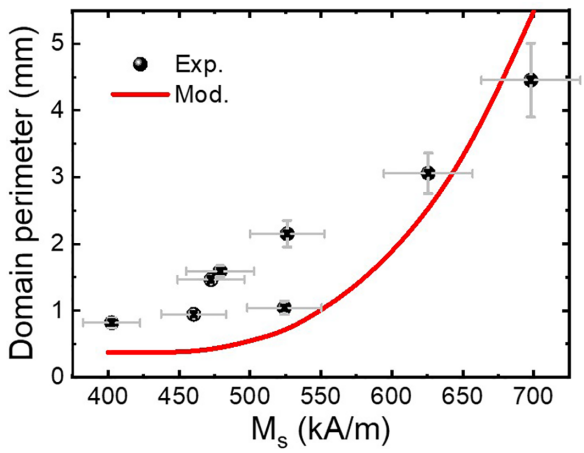

FIG. 3. Domain perimeter averaged over the four pulses versus saturation magnetization (black dots). Domain perimeter extracted from the theory of stable domain size versus saturation magnetization in stripe domains (red line).

The next step consisted of patterning dot arrays in the full film in order to bring the size of the structure below the equilibrium size of magnetic domains. Therefore, electron-beam lithography and dry argon etching were used to pattern dot arrays with a 3-μm diameter and 3.3-μm period. We chose the sample with the highest concentration of lutetium corresponding to the largest equilibrium domains. The 3-nm-thick $Co_{60}Lu_{40}$ kept its PMA after patterning.

As shown in Fig. 4(a), 531 dots are located in the region where the fluence is high enough to get magnetization reversal. After saturating the sample with a magnetic field, we shone a 50-fs laser pulse, then counted how many dots had their magnetization switched. After the first pulse, the magnetization of 263 dots switched from the M+ state to the M– state—namely, 49.5% of dots were switched by the femtosecond laser pulse. Meanwhile, 268 dots stayed in the M+ state. The second pulse made 139 dots switch from the M+ state to M– state and 114 dots switch from the M– state to the M+ state at the same time—namely, 47.6% of dots

TABLE I. Statistics for the single switching of the nanodot structure based on Fig. 4.

	$M+\rightarrow M-$	$M-\rightarrow M+$	Total	Switching rate
Pulse 0 to pulse 1	263	0	531	49.5%
Pulse 1 to pulse 2	139	114	531	47.6%
Pulse 2 to pulse 3	145	133	531	52.4%
Pulse 3 to pulse 4	143	129	531	51.2%

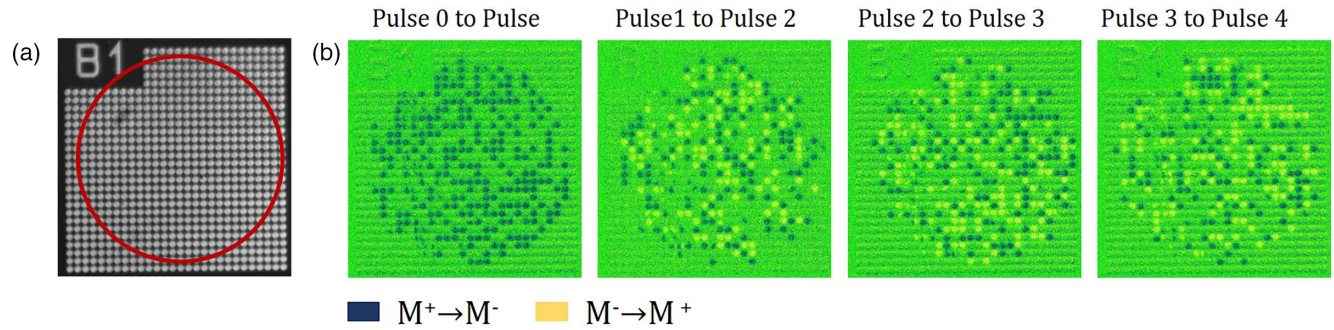

FIG. 4. Single-pulse reversal on the nanodot structure with a 3-μm dot diameter. (a) Nanodot arrays of a sample with a 40% lutetium concentration. The area enclosed by the red circle is the laser spot. (b) From left to right are the pictures that are subtracted by previous one. For example, pulse 0 to pulse 1 is image pulse 1 subtracted by the background, pulse 1 to pulse 2 is image pulse 2 subtracted by image pulse 1, and so on. Blue represents those dots that switched from the M+ state to M– state; yellow represents those dots that switched from M– state to M+ state. Experiments were done with a fluence of 9.3 mJ/cm^2.

switched. Thus, 243 dots stayed in the M+ state and 288 dots stayed in the M– state after pulse 2. As shown in Fig. 4(b) and Table I, more dots switched from the M+ state to the M– state, but fewer dots switched from the M– state to the M+ state. As a result, in comparison to $(CoFe)_xGd_{1-x}$, for which 100% of dots reverse, only ∼50% of dots can be switched by each laser pulse. Furthermore, and as a conclusion, the magnetization of each $Co_{60}Lu_{40}$ dot does not switch after each pulse.

III. DISCUSSION

The magnetic properties of $Co_{1-x}Lu_x$ alloys were promising to get single-shot reversal. Decreasing the thickness down to 3 nm, magnetization could be stabilized out of plane. Increasing the lutetium content, saturation magnetization could be decreased, allowing stabilization of micrometer-size domains and so single domain dots 3 μm in diameter. After a single laser pulse, the single domain state could be preserved, but reversal did not occur after each pulse. It appears that 50% of the dots reversed their magnetization after each pulse.

In order to shed light on this behavior, an atomistic simulation was performed. Since the magnetic parameters of lutetium are not well known, in a first step, static magnetization versus temperature was computed to adjust the magnetic parameters. The energy terms taken into account are the exchange energy given by a Heisenberg spin model and the anisotropy energy that includes the volume anisotropy linked to some crystallinity of the $Co_{1-x}Lu_x$ layer and the surface anisotropy due to the proximity of the platinum interfaces. We used the magnetic moment close to the one found in the literature, $\mu_{Lu} = 0.34\ \mu_B$/atom, and changed the exchange constant J_{Lu-Lu}. J_{Co-Lu} was fixed to -2×10^{-22}J and J_{Co-Co} to 4.8×10^{-21}J. Figure 5(a) shows the temperature-dependent magnetization evolution from which the Curie temperature of $Co_{1-x}Lu_x$ can be extracted for various lutetium concentrations (the polarization of platinum was not considered here). The evolution of magnetization as function of the temperature could be reproduced using $J_{Lu-Lu} = 6 \times 10^{-23}$J. The dynamics of the spin system was then computed based on the Langevin dynamics of the Landau-Lifshitz-Gilbert (LLG) equation, and the temperature of the spin system estimated with a two-temperature model that couples the spin and electron [17,24]. By means of the time integration of the LLG equation using the VAMPIRE software package [25], we can obtain the temporal evolution of a system of spins for different pulse fluences.

Figure 5(b) shows the laser fluence-dependent magnetization dynamics for $Co_{60}Lu_{40}$, with laser fluence changing from 6.5 to 10 mJ/cm^2. We can see that for all laser fluences, only demagnetization of the alloy could be obtained, as observed experimentally. A close analysis of magnetic moment versus temperature shows that, when temperature increases, the

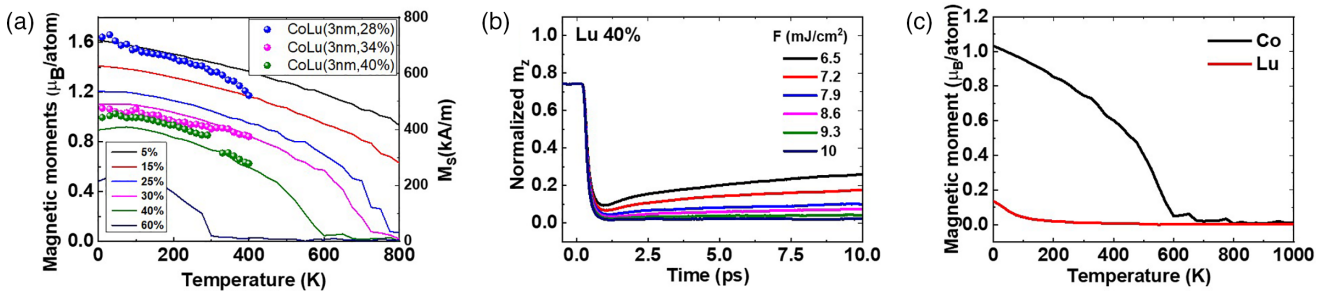

FIG. 5. (a) Magnetic moment versus temperature for $Co_{1-x}Lu_x$ alloys with various lutetium concentrations, x. Dots indicate experiments; lines indicate simulations. (b) Simulations of the cobalt demagnetization dynamics for the $Co_{60}Lu_{40}$ alloy as a function of laser power. (c) Simulations of the magnetic moment versus temperature for both cobalt and lutetium subnetworks in case of $Co_{60}Lu_{40}$.

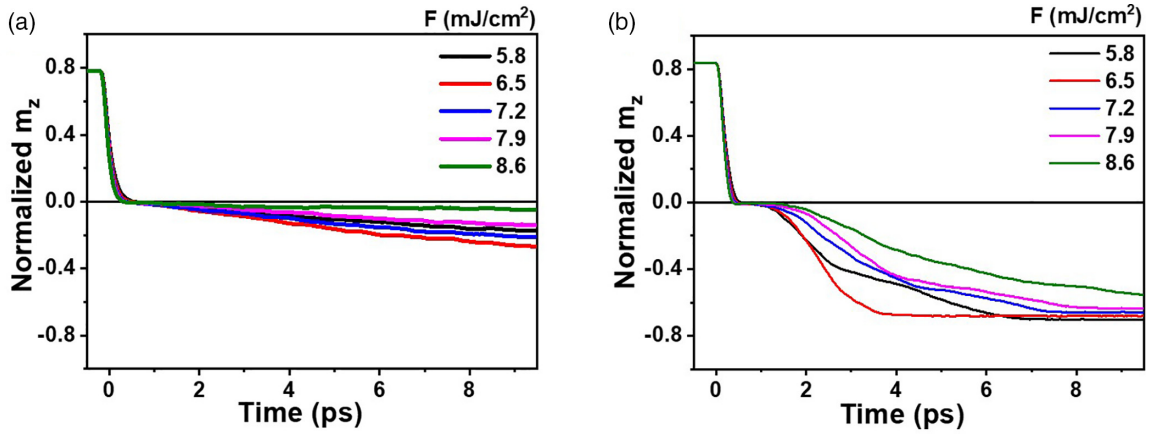

FIG. 6. (a) Demagnetization dynamics for $J_{\text{Lu-Lu}}$ equal to 6×10^{-22} J when $\mu_{\text{Lu}} = 4.34$ μ_B/atom as a function of fluence. (b) Demagnetization dynamics for $J_{\text{Lu-Lu}}$ equal to 6×10^{-21} J when $\mu_{\text{Lu}} = 3.34$ μ_B/atom as a function of fluence.

lutetium moment experiences a strong decrease and is close to zero, while the moment of cobalt only shows a decrease of 20%. As a result, for temperatures for which the reversal of cobalt could be activated, the angular momentum of lutetium is close to zero and no deterministic reversal can happen.

The magnetic parameter of lutetium (μ_{Lu} and $J_{\text{Lu-Lu}}$) has been varied in order to check if reversal could be observed. When $J_{\text{Lu-Lu}} = 6 \times 10^{-23}$J, the single-shot switching behavior cannot be observed, whatever the magnetic moment.

By increasing $J_{\text{Lu-Lu}}$ to 6×10^{-22}J, a value that remains two times lower then $J_{\text{Gd-Gd}}$ [17], magnetization switching occurs until $\mu_{\text{Lu}} = 4.34$ μ_B/atom, as shown in Fig. 6(a). Further increasing of $J_{\text{Lu-Lu}}$ leads to a decrease in this threshold. For example, Fig. 6(b) shows the magnetization switching behavior for $\mu_{\text{Lu}} = 3.34$ μ_B, when $J_{\text{Lu-Lu}} = 6 \times 10^{-21}$J. As a result, with its low magnetic moment per atom as well as its low Curie temperature, lutetium is not able to transfer enough angular moment or spin current to the cobalt subnetwork, leading to a nondeterministic magnetization reversal of the 3-μm-size dots.

In conclusion, while the magnetic properties of $Co_{1-x}Lu_x$ alloys were promising to get single-shot reversal, only nondeterministic reversal of 3-μm-diameter dots could be observed. The 50% reversal of dots with each pulse is consistent with the insufficient angular moment transfer from lutetium to the cobalt subnetwork.

ACKNOWLEDGMENTS

The authors acknowledge financial support from the ANR (Grant No. ANR-17-CE24-0007); the Region Grand Est through its FRCR call (NanoTeraHertz and RaNGE projects); the impact project LUE-N4S, part of the French PIA project "Lorraine Université d'Excellence" (Grant No. ANR-15IDEX-04-LUE); and the "FEDER-FSE Lorraine et Massif Vosges 2014–2020," a European Union Program.

[1] C. D. Stanciu, F. Hansteen, A. V. Kimel, A. Kirilyuk, A. Tsukamoto, A. Itoh, and T. Rasing, All-Optical Magnetic Recording with Circularly Polarized Light, Phys. Rev. Lett. **99**, 047601 (2007).

[2] C. H. Lambert, S. Mangin, B. S. D. Ch. S. Varaprasad, Y. K. Takahashi, M. Hehn, M. Cinchetti, G. Malinowski, K. Hono, Y. Fainman, M. Aeschlimann, and E. E. Fullerton, All-optical control of ferromagnetic thin films and nanostructures, Science **345**, 1337 (2014).

[3] S. Mangin, M. Gottwald, C. H. Lambert, D. Steil, V. Uhlíř, L. Pang, M. Hehn, S. Alebrand, M. Cinchetti, G. Malinowski, Y. Fainman, M. Aeschlimann, and E. E. Fullerton, Engineered materials for all-optical helicity-dependent magnetic switching, Nat. Mater. **13**, 286 (2014).

[4] I. Radu, K. Vahaplar, C. Stamm, T. Kachel, N. Pontius, H. A. Dürr, T. A. Ostler, J. Barker, R. F. L. Evans, R. W. Chantrell, A. Tsukamoto, A. Itoh, A. Kirilyuk, T. Rasing, and A. V. Kimel, Transient ferromagnetic-like state mediating ultrafast reversal of antiferromagnetically coupled spins, Nature (London) **472**, 205 (2011).

[5] T. A. Ostler *et al.*, Ultrafast heating as a sufficient stimulus for magnetization reversal in a ferrimagnet, Nat. Commun. **3**, 666 (2012).

[6] M. L. M. Lalieu, M. J. G. Peeters, S. R. R. Haenen, R. Lavrijsen, and B. Koopmans, Deterministic all-optical switching of synthetic ferrimagnets using single femtosecond laser pulses, Phys. Rev. B **96**, 220411 (2017).

[7] Y. Xu, M. Deb, G. Malinowski, M. Hehn, W. Zhao, and S. Mangin, Ultrafast magnetization manipulation using single femtosecond light and hot-electron pulses, Adv. Mater. **29**, 1703474 (2017).

[8] C. Banerjee, N. Teichert, K. Siewierska, Z. Gercsi, G. Atcheson, P. Stamenov, K. Rode, J. M. D. Coey, and J. Besbas, Single pulse all-optical toggle switching of magnetization without gadolinium in the ferrimagnet Mn_2Ru_xGa, Nat. Commun. **11**, 4444 (2020).

[9] L. Avilés-Félix, A. Olivier, G. Li, C. S. Davies, L. Álvaro-Gómez, M. Rubio-Roy, S. Auffret, A. Kirilyuk, A. V. Kimel, T. Rasing, L. D. Buda-Prejbeanu, R. C. Sousa, B. Dieny, and I. L. Prejbeanu, Single-shot all-optical switching of magnetiza-

tion in Tb/Co multilayer-based electrodes, Sci. Rep. **10**, 5211 (2020).

[10] M. Beens, M. L. M. Lalieu, A. J. M. Deenen, R. A. Duine, and B. Koopmans, Comparing all-optical switching in synthetic-ferrimagnetic multilayers and alloys, Phys. Rev. B **100**, 220409 (2019).

[11] V. López-Flores, N. Bergeard, V. Halté, C. Stamm, N. Pontius, M. Hehn, E. Otero, E. Beaurepaire, and C. Boeglin, Role of critical spin fluctuations in ultrafast demagnetization of transition-metal rare-earth alloys, Phys. Rev. B **87**, 214412 (2013).

[12] A. Ceballos, A. Pattabi, A. El-Ghazaly, S. Ruta, C. P. Simon, R. F. L. Evans, T. Ostler, R. W. Chantrell, E. Kennedy, M. Scott, J. Bokor, and F. Hellman, Role of element-specific damping in ultrafast, helicity-independent, all-optical switching dynamics in amorphous (Gd,Tb)Co thin films, Phys. Rev. B **103**, 024438 (2021).

[13] F. Givord and R. Lemaire, Proprietes cristallographiques et magnetiques des composes entre le cobalt et le lutecium, Solid State Commun. **9**, 341 (1971).

[14] K. Endo, M. Iijima, and A. Shinogi, The metamagnetic transition in pseudobinary Laves phase compounds $Lu(Co_{1-x}Al_x)_2$, J. Phys. Soc. Jpra **56**, 1316 (1987).

[15] G. Krill, J. P. Schillé, P. Sainctavit, C. Brouder, C. Giorgetti, E. Dartyge, and J. P. Kappler, Magnetic dichroism with synchrotron radiation, Phys. Scr. **T49A**, 295 (1993).

[16] M. S. S. Brooks, O. Eriksson, and B. J. Johansson, 3*d*-5*d* band magnetism in rare earth transition metal intermetallics: $LuFe_2$, J. Phys. Condens. Matter **1**, 5861 (1989).

[17] J. Wei, B. Zhang, M. Hehn, W. Zhang, G. Malinowski, Y. Xu, W. Zhao, and S. Mangin, All-Optical Helicity-Independent Switching State Diagram in Gd-Fe-Co Alloys, Phys. Rev. Appl. **15**, 054065 (2021).

[18] M. Hehn, S. Padovani, K. Ounadjela, and J.- P. Bucher, Nanoscale magnetic domain structures in epitaxial cobalt films, Phys. Rev. B **54**, 3428 (1996).

[19] C. Swindells, B. Nicholson, O. Inyang, Y. Choi, T. Hase, and D. Atkinson, Proximity-induced magnetism in platinum layered with rare-earth–transition-metal ferrimagnetic alloys, Phys Rev. Research **2**, 033280 (2020).

[20] M. El Hadri, M. Hehn, P. Pirro, C. Lambert, G. Malinowski, E. Fullerton, and S. Mangin, Domain size criterion for the observation of all-optical helicity-dependent switching in magnetic thin films, Phys. Rev. B **94**, 064419 (2016).

[21] V. Gehanno, Y. Samson, A. Marty, B. Gilles, and A. Chamberod, Magnetic susceptibility and magnetic domain configuration as a function of the layer thickness in epitaxial FePd (0 0 1) thin films ordered in the $L1_0$ structure, J. Magn. Magn. Mater. **172**, 26 (1997).

[22] U. Atxitia, D. Hinzke, O. Chubykalo-Fesenko, U. Nowak, H. Kachkachi, O. N. Mryasov, R. F. Evans, and R. W. Chantrell, Multiscale modeling of magnetic materials: Temperature dependence of the exchange stiffness, Phys. Rev. B **82**, 134440 (2010).

[23] L. Rózsa, U. Atxitia, and U. Nowak, Temperature scaling of the Dzyaloshinsky-Moriya interaction in the spin wave spectrum, Phys. Rev. B **96**, 094436 (2017).

[24] T. A. Ostler, R. F. L. Evans, R. W. Chantrell, U. Atxitia, O. Chubykalo-Fesenko, I. Radu, R. Abrudan, F. Radu, A. Tsukamoto, A. Itoh, A. Kirilyuk, Th. Rasing, and A. Kimel, Crystallographically amorphous ferrimagnetic alloys: Comparing a localized atomistic spin model with experiments, Phys. Rev. B **84**, 024407 (2011).

[25] R. F. L. Evans, W. J. Fan, P. Chureemast, T. A. Ostler, M. D. A. Ellis, R. W. Chanwell, J. Phys. Condens. Matter **26**, 103202 (2014).